Journal of Science and Technology – Engineering and Technology for Sustainable Development
Volume 36, Issue 1, March 2026, 032-038

A Study on the Influence of Ion Steric Effects in Electrodeposition

Van-Quyet Ngo, Van-Sang Pham*
School of Mechanical Engineering, Hanoi University of Science and Technology, Ha Noi, Vietnam
**Corresponding author email: sang.phamvan@hust.edu.vn*

Abstract

The study investigates the complex interactions of ions near the electrode surface, where phenomena such as ion overcrowding and overscreening significantly influence ion transport and electrokinetic behavior. Under the application of a large voltage, intense electrostatic forces act on ions near the electrode, causing substantial modifications to the electric double layer (EDL) structure and the spatial charge distribution. These effects are particularly pronounced in systems with high ionic concentrations, where steric hindrance and ion size disparities become critical. The classical Poisson-Nernst-Planck (PNP) model is inadequate for describing these phenomena, as it neglects steric effects and fails to account for ion-ion interactions in dense ionic environments. To overcome these limitations, the modified Poisson-Nernst-Planck (mPNP) model is employed. This model incorporates key factors such as ion size effects and ion-ion interactions, enabling the accurate simulation of phenomena including the formation of densely packed EDLs and ion dispersion under extreme conditions. Additionally, the mPNP equations are coupled with the Navier-Stokes equations to provide a comprehensive representation of ion transport and fluid dynamics. This integrated framework facilitates a deeper understanding of the interplay among electrostatic forces, fluid flow, and steric hindrance, offering critical insights into the behavior of electrochemical systems under high-voltage and high-concentration conditions.

Keywords: Electroconvective, finite-sized ions, modify PNP-NS, steric effect.

1. Introduction

The dynamics of electric double layers (EDLs) play a crucial role in many electrochemical systems, especially when subjected to high voltages, such as in AC electrophoresis applications. Traditional models, such as the classical Gouy-Chapman model, fail to accurately describe the behavior of EDLs under high voltage conditions (up to several volts, significantly higher than the thermal voltage, *kT/e* equal approximately 25 mV). This limitation is mainly due to the model's neglect of the finite size of ions, leading to unrealistic predictions of ion concentration near the electrode surface.

Various studies have been conducted to understand phenomena related to the finite size of ions (overcrowding effect) and electrostatic interactions (overscreening effect) in ionic liquids, Fig.1, particularly focusing on the structure and capacitance of the electric double layer (EDL) [1]. Experimental [2], theoretical [3], and simulation studies [4] have demonstrated that ionic liquids exhibit these effects. Kornyshev developed a modified Poisson-Boltzmann equation to describe the overcrowding effect based on statistical mechanics with a Fermi distribution [5], similar to Bikerman's model [6]. Kilic and colleagues [7] introduced a modified Nernst-Planck (mNP) equation to accurately predict steric effects in the ion transport dynamics between two parallel metal plates under an applied voltage. Furthermore, Bazant and collaborators [8] developed a modified Poisson equation to encompass both overscreening and overcrowding effects by incorporating the electrostatic correlation length to study the structure and capacitance of the EDL. The main impact of the finite ion size is to prevent unrealistic crowding of point ions. Instead, it forms a condensed layer of ions at the close-packed density limit, where each ion can include at least one surrounding hydration shell. Lee and colleagues [9] derived similar modified Poisson-Nernst-Planck (mPNP) equations by coarse-graining a simple lattice-based model that excludes interacting particles. Yochelis [10] applied the mPNP equations to analyze various characteristics of EDLs in ionic liquids, providing analytical conditions and applicable voltage limits, domain size, molecular packing, and short-range electrostatic correlation.

Beyond the structure and capacitance of EDLs, the dynamics of charging and electrokinetic flows are also crucial for ionic liquids. Thus, understanding the impact of overscreening and crowding effects on ion transport dynamics and the interaction between hydrodynamics, ion transport, and electrostatic forces is essential. To our knowledge, this topic has not been thoroughly explored in the existing literature.

Many studies have investigated the behaviour of electro convective flows on ion-selective surfaces with various geometries and under different voltage conditions. Among these, the focus has often been on chaotic ion transport and flow instability at high

p-ISSN 3093-3242
e-ISSN 3093-3579
https://doi.org/10.51316/jst.188.etsd.2026.36.1.5
Received: Jan 11, 2025; Revised: Aug 5, 2025
Accepted: Sep 24, 2025; Online: Feb 5, 2026.

voltages, as these phenomena are crucial for applications in electrodialysis and electrochemistry, including water purification, electrochemical machining, and microfluidic separation. In our previous studies [11, 12], conducted an in-depth analysis of ion transport combined with chaotic hydrodynamics on ion-selective surfaces in dilute electrolytes, using numerical solutions of the coupled Poisson-Nernst-Planck (PNP)-Navier-Stokes (NS) equations to replicate vortex flow structures and chaotic ion movement. Ibanez *et al.* experimentally investigated electrohydrodynamic instability at over limiting currents under high voltage.

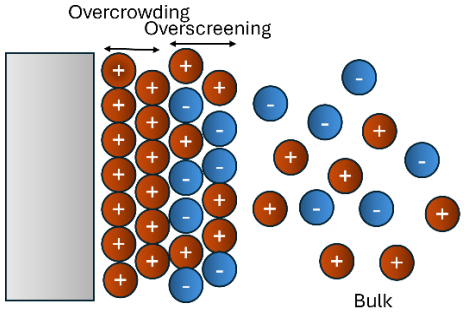

Fig. 1. Structure of electric double layer under high voltage conditions

In this work, we employ numerical simulations to solve the mPNP equations, as formulated by Bazant and collaborators [13], coupled with the Navier-Stokes equations. Our investigation focuses on four critical aspects to enhance the understanding of electric double-layer capacitor models and ion transport dynamics under high voltage conditions. First, we analyze the steric effects that limit double-layer charging in the mPNP framework. Second, we examine the current-voltage response to characterize the system's behavior across different applied potentials. Third, we investigate the structural changes within the electric double layer (EDL) induced by steric interactions. Finally, we explore the formation and evolution of vortex structures in the over limiting current regime, providing insights into the complex transport phenomena associated with high-voltage operation.

2. Modified Formulation

The modified PNP equations are based on the mean-field approximation and derived from the expression of the total free energy [14].

$$F = U - TS = \int d\boldsymbol{r}\left[-\frac{\varepsilon}{8\pi}|\nabla\varphi|^2 + z_1 e c_+\varphi + z_2 e c_-\varphi\right] - \frac{k_B T}{a^3}\int d\boldsymbol{r}[N_a c_+ a^3 \ln(N_a c_+ a^3) + N_a c_- a^3 \ln(N_a c_- a^3) + (1 - N_a a^3 c_+ - N_a a^3 c_-)\ln(1 - N_a a^3 c_+ - N_a a^3 c_-) \quad (1)$$

In (1), F denotes the Helmholtz free energy of the system, defined as $F = U - TS$, where U is the internal energy, T is the absolute temperature, and S is the entropy. The quantities z_+ and z_- are the valences of cations and anions, respectively, e is the elementary charge, and c_+ and c_- are the local number concentrations of cations and anions. The constant k_B is the Boltzmann constant, a is the effective ion size (cube root of the ionic volume), and N_a is Avogadro's number. The terms $N_a a^3 c_+$ and $N_a a^3 c_-$ represent the volume fractions of cations and anions, respectively, while $1 - N_a a^3 c_+ - N_a a^3 c_-$ denotes the volume fraction of the solvent.

$$\frac{\partial c_i}{\partial t} = D_i\nabla^2 c_i \pm D_i\frac{e}{k_B T}z_i\nabla\cdot(c_i\nabla\varphi) + N_a D_i a^3\cdot\nabla\cdot\left(\frac{c_i\nabla(c_+ + c_-)}{1 - N_a\cdot a^3\cdot c_1 - N_a\cdot a^3\cdot c_2}\right) - \mathbf{U}\cdot\nabla c_i. \quad (2)$$

In (2), $N_a D_i a^3\cdot\nabla\cdot\left(\frac{c_i\nabla(c_+ + c_-)}{1 - N_a\cdot a^3\cdot c_+ - N_a\cdot a^3\cdot c_-}\right)$ describes the steric effect of ions size. z_i represents the valence of each ion.

The chemical potentials can be obtained from the formula:

$$\mu_\pm = \frac{\partial F}{\partial c_\pm} = \pm ze\varphi - k_B T\ln c_\pm - k_B T\ln(1 - c_+ a^3 - c_- a^3) \quad (3)$$

In its dimensionless form, the electrochemical potential can be written as follows:

$$\mu_\pm = \ln\frac{c_\pm}{1 - v(c_+ + c_-)}, v = 2a^3 c_0 \quad (4)$$

Here $\mu_\pm$ are the regularized ionic electrochemical potentials, and v is the dimensionless ionic volume at zero voltage.

3. Theoretical Model and Method

3.1. Physical Setup

We investigate a two-dimensional open system featuring a single electrode surface subjected to an alternating current (AC) voltage, as depicted in Fig 2.

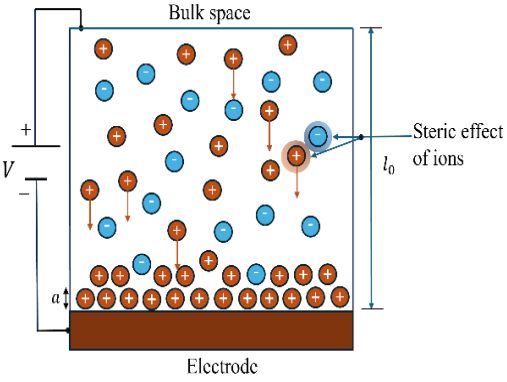

Fig. 2. Sketch of the model problem

3.2. Governing Equations and Boundary Conditions

3.2.1. Governing equations:

The transport of ions within the system is primarily governed by three mechanisms: the electric field, diffusion, and fluid convection. The modified Nernst–Planck equations describe the ion motion under these influences, incorporating three main components, migration driven by the electric field, diffusion caused by concentration gradients, and convection induced by fluid flow.

The coupling between the electric potential field and the ion concentration distribution is characterized by the Poisson equation, which defines the relationship between the ion density and the electric field generated by the charge distribution. This establishes a bidirectional feedback mechanism: variations in ion density alter the potential field, while the potential field simultaneously affects the ion transport process.

Meanwhile, the motion of the fluid responsible for convection is governed by the Navier–Stokes equations, which account for the effects of pressure forces, viscous forces, and other external influences to accurately describe the fluid dynamics within the system.

To simplify the analysis and improve generality, these governing equations are often expressed in dimensionless form. By introducing characteristic scales of length, time, and concentration, the number of parameters is reduced, allowing for a more transparent interpretation of the physical processes. The resulting dimensionless equations effectively capture the coupled behavior of ion transport, electric potential, and fluid flow in a unified and comprehensive framework.

The dimensionless form of these equations is as follows:

$$\frac{\partial c_{\pm}}{\partial t} = -\nabla \cdot \mathbf{J}_{\pm} \tag{5}$$

$$\mathbf{J}_{\pm} = c_{\pm}(-D_i \nabla \mu_{\pm} + Pe\mathbf{U}) \tag{6}$$

$$-\varepsilon^2 \Delta\phi = z_+ c_+ - z_- c_- \tag{7}$$

$$0 = -\nabla p + \Delta\varphi\nabla\varphi + \Delta\mathbf{U}, \qquad \nabla \cdot \mathrm{U} = \mathbf{0} \tag{8}$$

The above equations are all in dimensionless form with the corresponding reference values of concentration c_0, voltage V_0, velocity u_0, pressure p_0, average diffusion coefficient D_0, and electric field E_0.

$$c_0 = c_{bulk}, V_0 = \frac{k_B T}{ze}, u_0 = \frac{\varepsilon_0 \varepsilon_r V_0^2}{\eta l_0},$$
$$p_0 = \frac{\eta u_0}{l_0}, D_0 = \frac{D_+ + D_-}{2}, E_0 = \frac{V_0}{l_0} \tag{9}$$

where c_0 is the concentration scale, l_0 is the characteristic length scale, D_0 is the average diffusion, η is the dynamic viscosity of the solution. Value of the potential scale (V_0) and ion current scale (I_0) 25.85 mV, 1.62 mA, respectively.

The system is characterized by the dimensionless Debye length ε. In this study, ε equal $2 \cdot 10^{-4}$, corresponds to the characteristic length l_0 equal 60 μm, bulk concentration C_0 equal 1 mM (NaCl), and absolute temperature T equal 300 K. Other parameters used in the simulation include the diffusivities D_+ equal $1.33 \times 10^{-9}\ m^2 s^{-1}$ and D_- equal $2.03 \times 10^{-9}\ m^2 s^{-1}$.

3.2.2. Boundary conditions:

For closure of the governing equations, boundary conditions are also supplied. At the electrode surface, no-flux conditions is enforced to anions; interface concentration p_1 equal 10000 [13], the common no-slip boundary condition is enforced to the fluid . At the bulk space, ionic species are well mixed, C_+ equal C_- equal 2, Bias voltage is applied to the system through a fixed-value bounday condition for electric potential at top boundary (φ equal 0) and the bottom boundary (φ equal $-V$). At other boundaries, all variables are assumed to be periodic.

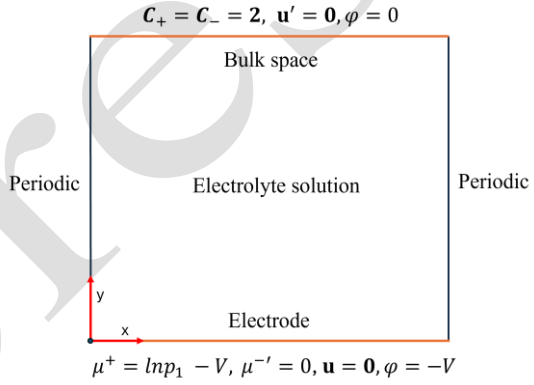

Fig. 3. Computational domain

3.2. Numerical Methods

Simulations were performed using an in-house code, which solved the modified Poisson-Nernst-Planck-Navier-Stokes (mPNP-NS) equations directly on a two-dimensional domain. The mPNP and NS equations are connected in a nonlinear manner. The convection term in the mPNP equations and the electric body force in the NS equations serve as the links between these two sets of equations. We developed a coupled approach to solve the mPNP and NS equations to avoid solving a complicated system of linear equations and ensure the strong coupling of the mPNP and NS equations. In this approach, the potential and ion concentrations are simultaneously solved from the mPNP equations, starting with the velocity field from the previous iteration or initial condition. The boundary conditions at the electrode surface are adjusted to accurately reflect the finite size of ions. The NS equations are then modified to include the electric body force. The mPNP equations are updated using the velocity field obtained from the solution of the NS equations. This procedure is repeated until convergence, as illustrated in Fig. 4.

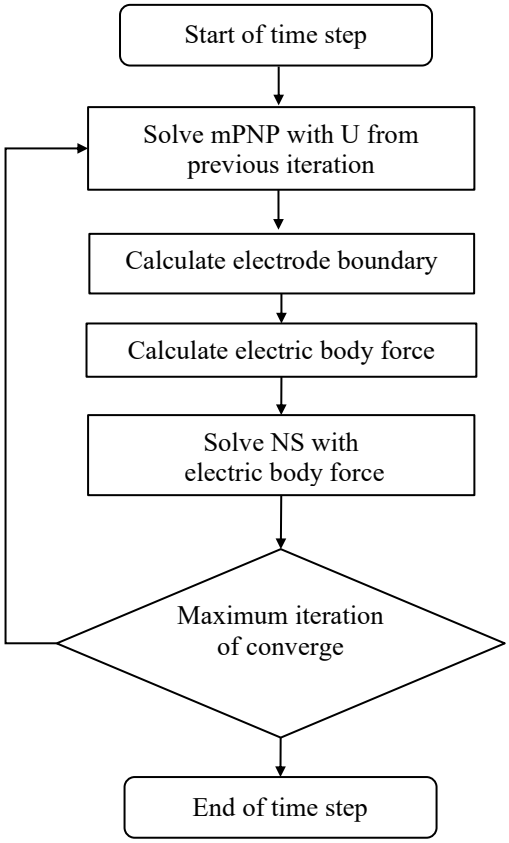

Fig. 4. The flow chart of simulation algorithm

The equations are discretized using the locally conservative finite volume method. The Newton-Raphson method is used to solve the nonlinear discretized mPNP equations. The finite-element mesh generator (GMSH) is used to refine the mesh near the electrodes due to the rapid changes in ion concentrations and electric potential within the electrical double layer (EDL).

A mesh of 8400 cells was used to represent the computation domain (Fig. 3). The smallest mesh size is 4.73×10^{-7}, for the cells next to the electrode's surfaces. All simulations were conducted using the M4800 Dell workstation with Intel i7, 2.4 Gh, processor, and 8 Gb of RAM. Time-consuming happens mostly at the modified Poisson-Nernst-Planck equations solver. Validations for the numerical solver can be found in our previous works [11, 15].

4. Results and Discussion

4.1. Steric Limit in Double Layer Charging for mPNP Model

The results in Fig. 5. illustrate the difference in total charge within EDL. The dashed blue line represents the solution obtained using the classical PNP model at v equal 0, while the solid green and red lines represent the solution from the mPNP model. For clarity, we examined cases with extreme steric restriction at 0.2 and v equal 0.25. Here, the applied voltage exceeds ten times the thermal voltage ($V = 10V_0$). Under such conditions, the mPNP model clearly shows that ion concentration is constrainded by steric limit, which is defined as $1/v$. In contrast, the classical PNP model predicts an exponential increase in ion concentration. The divergence between these two models can be explained by the phenomenon of ion crowding. In the mPNP model, the steric effects impose a physical limit on the total ion concentration in a unit volume, restricting it to $1/v$. This reflects the reality that ions cannot occupy the same physical space beyond a certain packing density. On the other hand, the classical PNP model does not account for steric effects and therefore allows ion concentrations to increase indefinitely, leading to unrealistic predictions at high voltages.

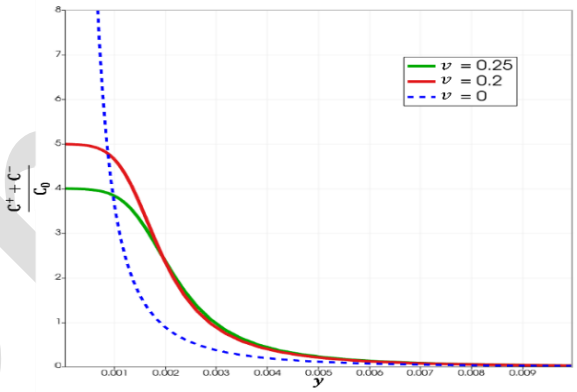

Fig. 5. The dimensionless total ion concentration near the boundary at $y = 0$

4.2. Current-Voltage Response

The current-voltage response in different cases is presented in Fig. 6: the classical model for point-like ions with v equal 0; intermediate steric restriction with v equal 10^{-3} (corresponding to a maximum ionic concentration of approximately 10 M for a 10 mM bulk solution); severe steric restriction with v equal 10^{-2} (1 Molar maximum ionic concentration for a 10 mM bulk solution); and extreme steric restriction with v equal 0.1 and v equal 0.2 [11].

The value of v increases progressively from v equal 0 (solid line with circle), v equal 0.001 (dashed line with square), v equal 0.01 (dash-dot line with triangle), v equal 0.1 (dotted line with diamond) and v equal 0.2 (solid line with x marker). The curve is divided into two distinct regions: the Ohmic region, the limiting current region

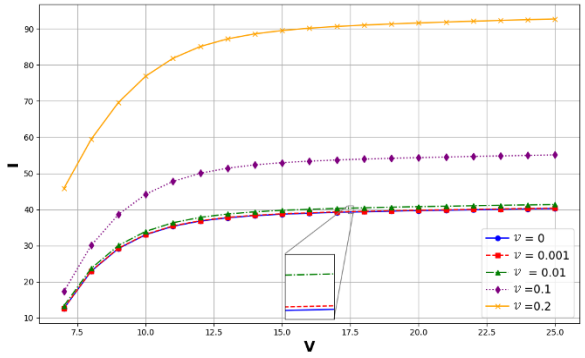

Fig. 6. The current-voltage (I-V) curves for 5 cases with varying degrees of steric hindrance, characterized by the parameter v

In the Ohmic regime, when the applied voltage is low ($V \leq 15V_0$), the current increases linearly with the applied voltage in all cases. When there are still many ions near the electrode, the number of increases as the voltage rises, leading to an increase in current, primarily due to the diffusion of counter-ion and a decrease in ion concentration at the electrode surface. Steric effect has a significant impact on the electrical conductivity of the system. As the voltage increases, the slope of the current-voltage curve also increases, reflecting changes in the mobility of ions that are hindered by the steric effect.

For the steric coefficient (v) 0.001 and 0.01, the current density through the electrode does not change significantly. The current density reaches its peak value of approximately 40 (A/m^2) at V equal 15 V_0. These steric effects show no significant difference compared to the classical model ($v = 0$). However, when v increase, especially at v equal 0.1 and v equal 0.2, the impact of the steric effect becomes more pronouncd. This lead to significant changes in ion distribution and the mobility of ions causing a marked increase in current density. Specifically, the magnitude of current reaches approximately 52 (A/m^2) at v equal 0.1 and 90 (A/m^2) at v equal 0.2. Although the steric effect restricts the mobility of ions in the system, it also leads to the accumulation of counter-ions at the electrode surface. Higher ion density creates a region near the electrode with a larger number of charge carriers, thereby increasing the electrical conductivity of the system.

In the limiting current regime, which occurs at higher applied voltages ($V \geq 15V_0$), the ion concentration at the electrode surface diminishes significantly, approaching zero. In this regime, further increase in applied voltage do not result in aproportional increase in current. This phenomenon is attributed to the depletion of ions, which act as charge carriers, near the electrode surface. While the steric effect continues to influence ion mobility and distribution, the absence of sufficient ions near the surface becomes primary limiting factor for current increase.

4.3. The structural change of the EDL is influenced by steric effects

Fig. 7. illustrates the distribution of cation concentration (C_+) within the EDL under varying levels of steric hindrance. When v is equal 0, representing the absence of steric effects, the ion concentration exhibits a sharp peak near the electrode surface, resulting in a thin electric double layer. This behavior aligns with the classical Poisson-Nernst-Planck model, which assumes point-like ions and neglects their finite size and spatial interactions.

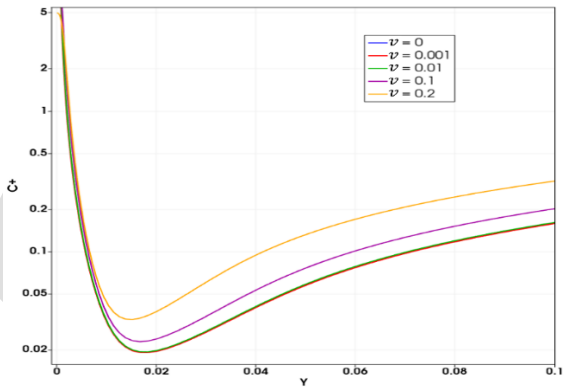

Fig. 7. The distribution of cation concentration along the Y-axis at $V = 20\ V_0$, which is perpendicular to the electrode, for the different levels of steric hindrance ($v = 0$ to 0.2)

As the value of v increases, steric effects begin to significantly influence ion distribution. At higher values, such as v equal 0.1 and v equal 0.2, the ion concentration near the electrode surface decreases substantially. This reduction arises from the finite size of the ions, which restricts their accumulation near the surface. This phenomenon also leads to a pronounced increase in the thickness of the EDL, clearly illustrating the "crowding" effect, where ions experience spatial competition and strong interactions. Additionally, the ion concentration in regions farther from the electrode increases with higher v, resulting in a more uniform distribution of ions throughout the EDL.

The observed changes in ion distribution with increasing steric effects underscore the importance of accounting for ion size and spatial interactions when characterizing the structure of the EDL. This effect is particularly critical under high voltage conditions, where ions are strongly influenced by the electric field and tend to over-accumulate near the electrode if steric

effects are neglected. The findings emphasize the necessity of employing advanced models, such as the mPNP model, to provide an accurate description of the electric double layer structure under complex electrochemical conditions.

Fig. 8. provides a detailed comparison of extended space charge (ESC) layer structure near the electrode under overlimiting conditions, illustrating the impact of steric effects. The solid line (mPNP) represents the case where steric effects are included, while the dashed line (PNP) corresponds to the case without steric effects. The comparison reveals significant differences in the spatial distribution of charge density (ρ_e) caused by the presence of steric effects.

Near the electrode surface, both models predict high charge density, reflecting the accumulation of ions under the influence of a strong electric field. However, moving away from the electrode, the ESC layer becomes noticeably wider when steric effects are considered, with ρ_e exhibiting a slower decay. This extended profile arises from steric hindrance, which redistributes ions and modifies their packing dynamics within the EDL.

Additionally, steric effects lead to the emergence of a distinct second peak in ρ_e, indicating greater overlap of the inner EDL layers. When steric effects are neglected, the ESC layer still forms but remains more confined, and ρ_e decays more rapidly.

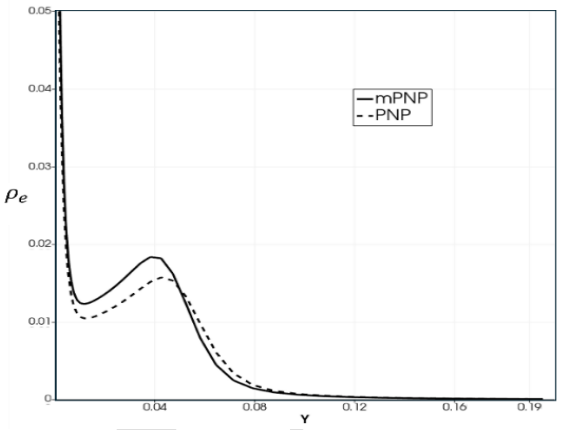

Fig. 8. Comparison of the extended space charge profile near the electrode in overlimiting regimes: with and without steric effects at V equal $30V_0$

4.4. The vortex Structure in the Overlimiting Regime

When the voltage difference exceeds the critical valueV_{cr} equal of 31, the seed vortices are disupted due to the distortion effect, which is the result of the electric field acting on the charge in the expanded electric double layer.

In Fig. 9, the seed vortices begin to break apart and subsequently merge into larger vortices. Similar to the seed vortices, each large vortex rotates in the opposite direction to its adjacent vortices.

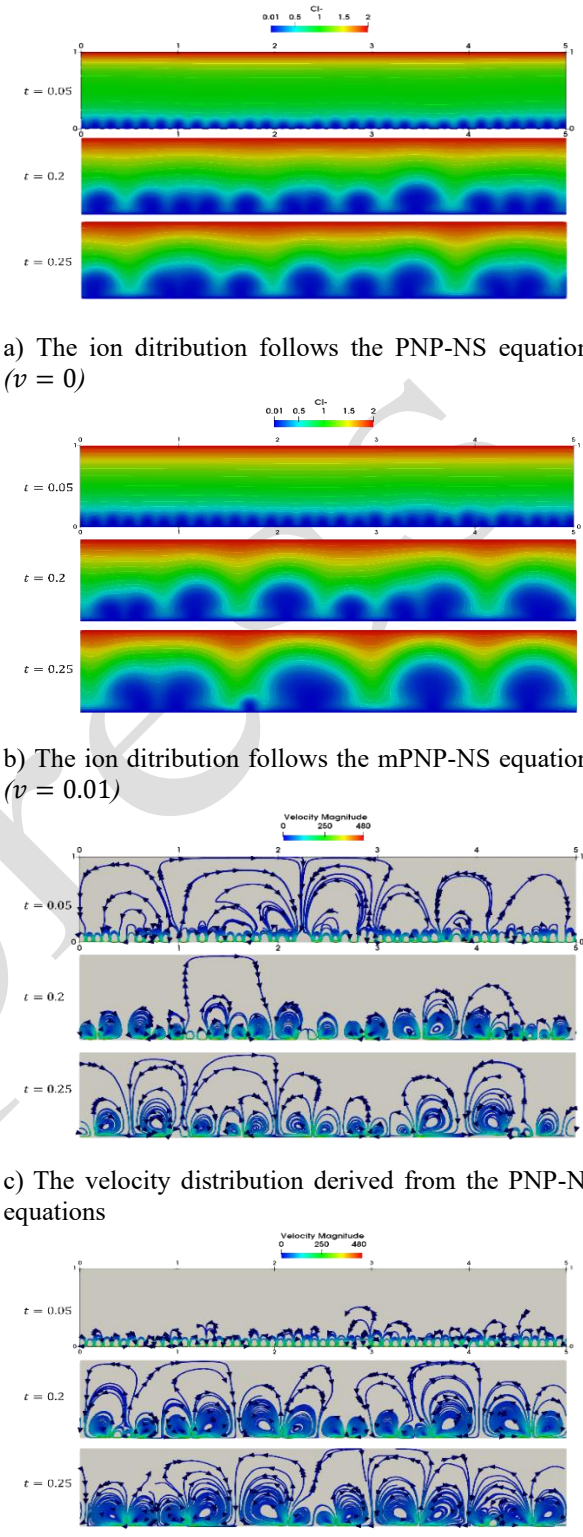

a) The ion ditribution follows the PNP-NS equations *($v = 0$)*

b) The ion ditribution follows the mPNP-NS equations *($v = 0.01$)*

c) The velocity distribution derived from the PNP-NS equations

d) The velocity distribution derived from the mPNP-NS equations

Fig. 9. Distribution of ion concentration c_ and velocity in electroconvective flow near electrode surface: Comparison between cases with and without considering the steric effect (overlimiting current, $V = 33\ V_0$) over a time series

The formation of these larger vorticers facilitates the transport of fluid with high ion concentration from the region outside the depletion zone towards the electrode surface. To investigate the influence of steric effects on this transport process, we compare the predictions of the PNP-NS (a) and mPNP-NS (b) equations with a time step Δt equal 0.001 and v equal 0.01.

From Fig. 9, it can be observed the the process of seed vortex breakup and merging occurs more rapidly in the case with steric effects. Specifically, at time t equal 0.2, when steric effects are not considered, the number of visible vortex pairs is 12, while in the case (b), only 7 vortex pairs are present, and their sizes are larger. At t equal 0.25, the vortices in the case (b) have nearly stabilized, but in case (a), without steric hindrance, the vortices have not fully stabilized yet.

5. Conclusion

By using numerical methods to solve the modified Poisson-Nernst-Planck (mPNP) equations coupled with the Navier-Stokes equations, we investigated the effects of considering the finite volume of ions. A notable advantage of the mPNP equations is their ability to handle high voltage levels effectively by avoiding the exponential increase in ion concentration predicted by classical PNP equations, which poses significant numerical challenges. Instead, the mPNP equations provide more realistic ion concentration profiles at all voltage levels and offer more accurate predictions within the electric double layer (EDL), where high ion density and significant ion-ion interactions occur. Additionally, our results reveal key phenomena, including changes in conductivity on the I-V curve, the formation of vortex flows, and the ion concentration limits within the system. These findings underscore the potential of the mPNP equations in simulating and analyzing complex electrochemical systems, particularly under conditions where traditional PNP equations prove inadequate.

References

[1] D. Lee, D. Im, and I. Kang, Electric double layer at the interface of ionic liquid–dielectric liquid under electric field, Langmuir, vol. 29, iss. 6, pp. 1875–1884, Jan. 2013. https://doi.org/10.1021/la3040775

[2] M. T. Alam, M. M. Islam, T. Okajima, and T. Ohsaka, Measurements of differential capacitance at mercury/room-temperature ionic liquids interfaces, The Journal of Physical Chemistry C, vol. 111, iss. 49, pp. 18326–18333, Nov. 2007. https://doi.org/10.1021/jp0758081

[3] Y. Levin, Electrostatic correlations: from plasma to biology, Reports on Progress in Physics, vol. 65, pp. 1577–1632, Sep. 2002. https://doi.org/10.1088/0034-4885/65/11/201

[4] M. V. Fedorov and A. A. Kornyshev, Towards understanding the structure and capacitance of electrical double layer in ionic liquids, Electrochimica Acta, vol. 53, iss. 23, pp. 6835–6840, Oct. 2008. https://doi.org/10.1016/j.electacta.2008.02.065

[5] A. A. Kornyshev, Double-layer in ionic liquids: paradigm change, The Journal of Physical Chemistry B, vol. 111, iss. 20, pp. 5545–5557, May 2007. https://doi.org/10.1021/jp067857o

[6] J. J. Bikerman, Structure and capacity of electrical double layer, London, Edinburgh, and Dublin Philosophical Magazine and Journal of Science, vol. 33, iss. 220, pp. 384–397, Apr. 1942. https://doi.org/10.1080/14786444208520813

[7] M. S. Kilic, M. Z. Bazant, and A. Ajdari, Steric effects in the dynamics of electrolytes at large applied voltages. I. double-layer charging, Physical Review E, vol. 75, no. 2, Art. no. 021502, Feb. 2007. https://doi.org/10.1103/PhysRevE.75.021502

[8] M. Z. Bazant, B. D. Storey, and A. A. Kornyshev, Double layer in ionic liquids: overscreening versus crowding, Physical Review Letters, vol. 106, no. 4, Jan. 2011, Art. no. 046102. https://doi.org/10.1103/PhysRevLett.106.046102

[9] A. A. Lee, S. Kondrat, D. Vella, and A. Goriely, Dynamics of ion transport in ionic liquids, Physical Review Letters, vol. 115, Sep. 2015, Art. no. 106101. https://doi.org/10.1103/PhysRevLett.115.106101

[10] A. Yochelis, Spatial structure of electrical diffuse layers in highly concentrated electrolytes: a modified poisson–nernst–planck approach, The Journal of Physical Chemistry C, vol. 118, iss. 11, pp. 5716–5724, Mar. 2014. https://doi.org/10.1021/jp412616f

[11] V. S. Pham, Z. Li, K. M. Lim, J. K. White, and J. Han, Direct numerical simulation of electroconvective instability and hysteretic current-voltage response of a permselective membrane, Physical Review E, vol. 86, no. 4, Oct. 2012, Art. no. 046310. https://doi.org/10.1103/PhysRevE.86.046310

[12] V. S. Pham, H. Kwon, B. Kim, J. K. White, G. Lim, and J. Han, Helical vortex formation in three-dimensional electrochemical systems with ion-selective membranes, Physical Review E, vol. 93, no. 3, Mar. 2016, Art. no. 033114. https://doi.org/10.1103/PhysRevE.93.033114

[13] I. Rubinstein and B. Zaltzman, How the fine structure of the electric double layer and the flow affect morphological instability in electrodeposition, Physical Review Fluids, vol. 8, Sep. 2023, Art. no. 093701. https://doi.org/10.1103/PhysRevFluids.8.093701

[14] I. Borukhov, D. Andelman, and H. Orland, Steric effects in electrolytes: a modified Poisson–Boltzmann equation, Physical Review Letters, vol. 79, no. 3, pp. 435–438, Jul. 1997. https://doi.org/10.1103/PhysRevLett.79.435

[15] Q. V. Do, D. A. Van, V. B. Nguyen, and V. S. Pham, A numerical modeling study on inertial focusing of microparticle in spiral microchannel, AIP Advances, vol. 10, iss. 7, Jul. 2020, Art. no. 075017. https://doi.org/10.1063/5.0006975